JACS
JOURNAL OF THE AMERICAN CHEMICAL SOCIETY
Article
pubs.acs.org/JACS

Anti-Fab Aptamers for Shielding Virus from Neutralizing Antibodies

Darija Muharemagic,[†] Mahmoud Labib,[†] Shahrokh M. Ghobadloo,[†] Anna S. Zamay,[†,‡] John C. Bell,[§,∥] and Maxim V. Berezovski*[,†]

[†]Department of Chemistry, University of Ottawa, 10 Marie Curie, Ottawa, Ontario K1N 6N5, Canada

[‡]Institute of Molecular Medicine and Pathological Biochemistry, Krasnoyarsk State Medical University, 1 P. Zheleznyaka str., Krasnoyarsk 660022, Russia

[§]Department of Biochemistry, Microbiology and Immunology, Faculty of Medicine, University of Ottawa, 501 Smyth Road, Ottawa, Ontario K1H 8L6, Canada

[∥]Jennerex Inc., 450 Sansome Street, 16th floor, San Francisco, California 94111, United States

Supporting Information

ABSTRACT: Oncolytic viruses are promising therapeutics that can selectively replicate in and kill tumor cells. However, repetitive administration of viruses provokes the generation of neutralizing antibodies (nAbs) that can diminish their anticancer effect. In this work, we selected DNA aptamers against the antigen binding fragment (Fab) of antivesicular stomatitis virus polyclonal antibodies to shield the virus from nAbs and enhance its in vivo survival. For the first time, we used flow cytometry and electrochemical immunosensing to identify aptamers targeting the Fab region of antibodies. We evaluated the aptamers in a cell-based infection assay and found that several aptamer clones provide more than 50% shielding of VSV from nAbs and thus have the potential to enhance the delivery of VSV without compromising the patient's immune system. In addition, we developed a bifunctional label-free electrochemical immunosensor for the quantitation of aptamer-mediated degree of shielding and the amount of vesicular stomatitis virus (VSV) particles. Electrochemical impedance spectroscopy was employed to interrogate the level of VSV in a linear range from 5×10^4 to 5×10^6 PFU mL^{-1} with a detection limit of 10^4 PFU mL^{-1}.

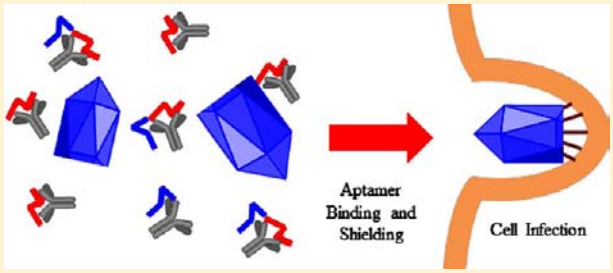

INTRODUCTION

Viral-based therapeutics hold great promise for the treatment of many diseases, especially cancer at the cellular level.[1] Vesicular stomatitis virus (VSV) is an arthropod-borne, negative-stranded RNA virus that primarily affects rodents, cattle, swine, and horses, but can also infect human and other species.[2] A number of studies have alternatively demonstrated that defects in antiviral innate immune responses involving the interferon system play a prominent role in allowing VSV to robustly replicate in tumor cells, thus invoking cytolysis.[3] Conversely, VSV replication in normal cells is usually thwarted by the innate immune response. VSV as an oncolytic virus (OV) administered intravenously can be particularly effective against metastatic cancers, which are difficult to treat via conventional therapy. In vivo trials demonstrated that OVs can be deactivated by neutralizing antibodies (nAbs) and rapidly cleared from the circulation.[4] Therefore, a prerequisite for successful virotherapy is that the virus must gain access to tumor cells, which requires an extended circulation time without depletion by nAbs. Current approaches to extend circulation time employ polymer-coating technologies with poly-[*N*-(2-hydroxypropyl) methacrylamide] (HPMA)[5] and polyethylene glycol (PEG)[6] or use preinfected T cells as carriers for oncolytic viruses to tumor sites.[7] However, the use of polymer coating does suffer from substantial drawbacks as the polymer coating is permanent and thereby decreases infectivity. The other method requires isolation of patient's T cells, their activation, followed by back-infusion to the patient, which makes it impractical for clinical use. Development of aptamers binding to nAbs seems promising in terms of shielding the virus from nAbs with aptamers that could allow the virus to escape the host immune mechanism and neutralization. This can be feasible if an aptamer can be selected to an antigen-binding fragment (Fab) of nAbs. Antibodies can exist in two physical forms, a soluble form that is secreted from plasma B cells, and a membrane-bound form that is attached to the surface of B cells and is referred to as the B cell receptor.[8] When the B cell receptor encounters an antigen such as an oncolytic virus, this will lead to the activation of these cells and their subsequent differentiation into either antibody producing cells called plasma cells or memory B cells. Ideally, aptamers should bind to soluble antibodies, and this binding can be tested using flow cytometry and cell-based assays. On the other hand, aptamers should also have a high affinity to immobilized antibodies or B cell receptors so that they can prevent their binding to the respective oncolytic virus. This would block the differentiation of B cells into plasma cells

Received: July 13, 2012
Published: September 27, 2012

dx.doi.org/10.1021/ja306856y | J. Am. Chem. Soc. 2012, 134, 17168−17177

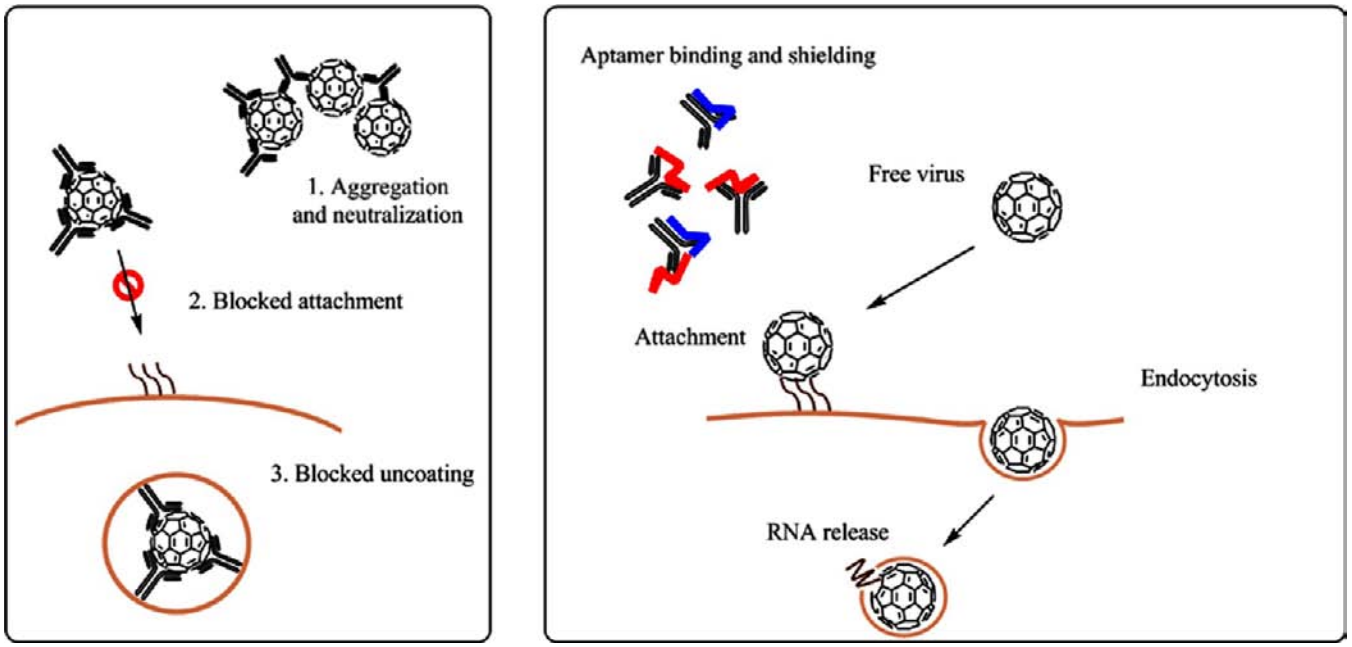

Figure 1. Principle of aptamer-mediated neutralizing antibody shielding (AptaNAS). (A) Anti-VSV neutralizing antibodies bind to the virus, which causes aggregation, block the attachment of the virus to the cell membrane, or prevent uncoating of the virus inside the cell. (B) With aptamers binding to the Fab fragment of antibodies, the virus is free to infect a cell.

and subsequently stop expressing the neutralizing antibodies against the virus.

In this work, we developed aptamer-mediated neutralizing antibody shielding (AptaNAS) technology to enhance survival of oncolytic viruses and efficiency of anticancer treatment, as schematically depicted in Figure 1. We selected aptamer pools and clones specific to rabbit anti-VSV neutralizing polyclonal antibodies (nAbs) and evaluated their binding affinities to Fab using flow cytometry and electrochemical sensing. We applied a bifunctional electrochemical immunosensor for the quantitative detection of VSV and measurement of the degree of shielding (DoS) of selected aptamers. In addition, aptamers with high DoS values were tested in a cell-based plaque forming assay to evaluate their biological activity; the aptamers prevented in vitro neutralization of VSV by nAbs and significantly increased the virus infection rate of cells.

EXPERIMENTAL SECTION

Virus. Vesicular stomatitis virus is a recombinant virus with a deletion of methionine 51 in the M protein (VSVΔ51), as well as an extra cistron encoding green fluorescent protein (GFP) inserted between the G and L sequences.[9] The virus replication is thought to be regulated by interferon (IFN) signaling, which is defective in most tumors. The mutant strain exploits this tumor-specific defect to enhance tumor targeting and minimize virus replication in normal cells. The virus was propagated in Vero African green monkey kidney cells, as described previously.[10]

DNA Library and Primers. The 80nt DNA library contained a central randomized sequence of 40nt flanked by 20nt primer hybridization sites (5′-CTC CTC TGA CTG TAA CCA CG-$(N)_{40}$-GCA TAG GTA GTC CAG AAG CC-3′). The 5′-primer labeled with a fluorescent dye (5′-/6-FAM/CTC CTC TGA CTG TAA CCA CG-3) and the nonlabeled 3′-primer (5′-GGC TTC TGG ACT ACC TAT GC-3′) were used in PCR reactions for the synthesis of single-stranded DNA. Nonlabeled 5′- and 3′-primers were used for PCR reactions to generate double-stranded DNA used for cloning. All oligonucleotides were synthesized by Integrated DNA Technologies (IA).

Magnetic Beads. Pure Proteome Protein G Magnetic Beads and Pure Proteome Magnetic Stand were purchased from Millipore (MA) and were suspended and washed in Dulbecco's Phosphate Buffered Saline (DPBS) from Sigma-Aldrich (Ontario, Canada). Beads were incubated with rabbit serum containing 3.5 mg mL^{-1} of polyclonal anti-VSV neutralizing antibodies (nAbs) (Jennerex, Ontario, Canada) at room temperature for 15 min with continuous mixing. The presence of nAbs on beads was confirmed by incubating the beads with 10 ng μL^{-1} of Alexa Fluor 488 chicken antirabbit IgG (H+L) (Invitrogen, CA); the fluorescence of the beads was monitored with a Gallios flow cytometer (Beckman Coulter, CA) and analyzed with FlowJo software (OR).

Aptamer Selection. DNA library was denatured at 95 °C for 5 min and then snap cooled on ice for 10 min. The DNA library (200 nM in 50 μL) was then incubated with 5×10^5 beads coupled with anti-VSV nAbs for 1 h at room temperature and continuous mixing. To separate bound from unbound DNA, the beads were washed three times with DPBS. Bound DNA was then eluted from the beads by denaturing at 85 °C for 10 min. For the first five rounds, we performed a positive selection followed by a negative selection step to protein G magnetic beads where the eluted DNA was mixed with the beads alone. The solution was incubated, with continuous mixing, for 1 h at room temperature. Unbound DNA was collected and amplified by symmetric and asymmetric PCR reactions. The asymmetric product was then concentrated and purified by Nanosep Centrifugal Devices (Pall, NY) and used for a following round of selection. In rounds 6–10, beads for negative selection steps were coupled with non-VSV antibodies prior to their incubation with the eluted DNA. In rounds 11–15, two negative selections, beads alone and beads with nonspecific antibodies, respectively, preceded the positive selection step. Next, unbound DNA was collected and used for incubation with anti-VSV nAbs coupled with magnetic beads.

The affinity of aptamers to nAb-coated beads during the selection was monitored using flow cytometry. A total of 150 nM of 6-FAM-labeled DNA, obtained from asymmetric PCR amplification after each selection round, was continuously mixed with magnetic beads coupled with nAbs for 1 h at room temperature. Following the incubation step, the beads were washed, resuspended in 250 μL of DPBS buffer, and subjected to flow cytometric analysis.

dx.doi.org/10.1021/ja306856y | J. Am. Chem. Soc. 2012, 134, 17168–17177

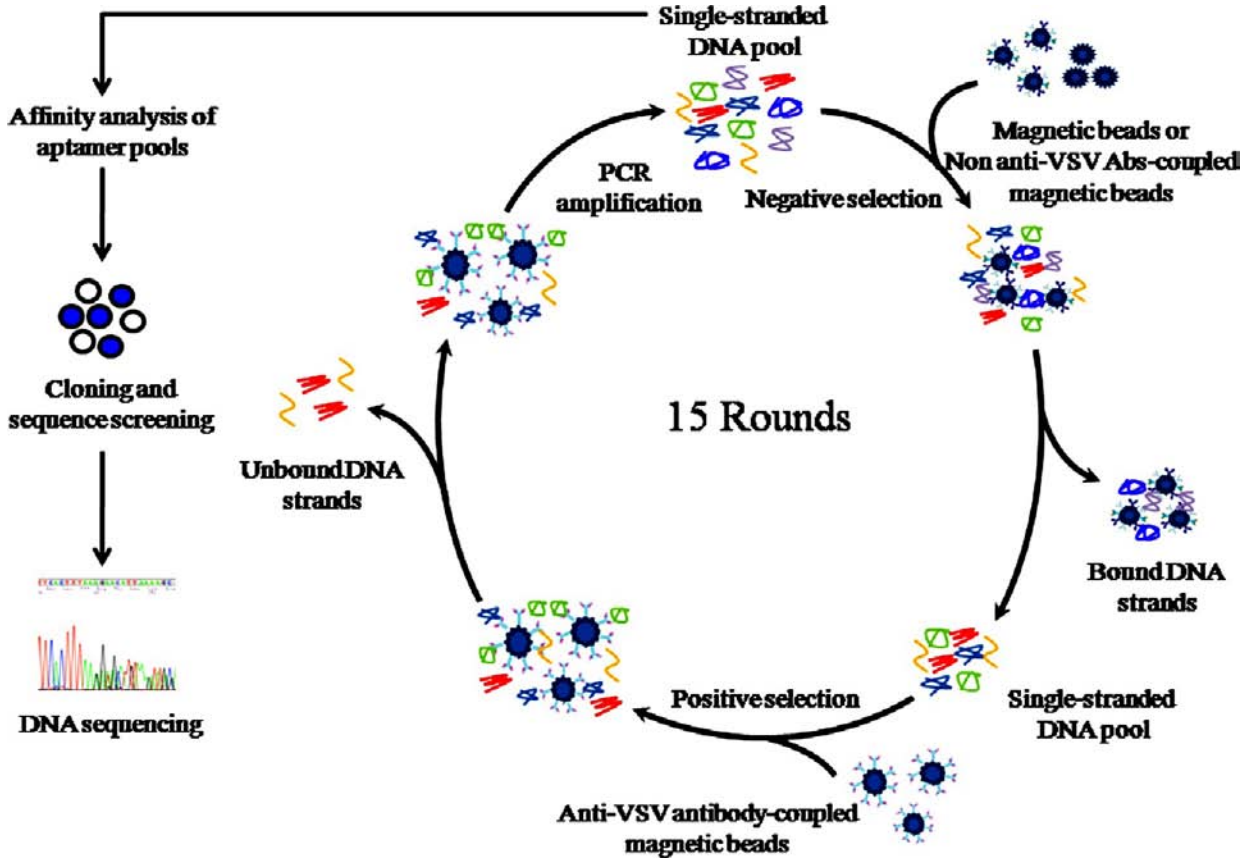

Figure 2. Selection of DNA aptamers to virus neutralizing antibodies. The SELEX procedure consists of 15 rounds iterating three major steps: (i) negative selection to magnetic beads and non-VSV Abs on beads, (ii) positive selection to anti-VSV Abs on beads, and (iii) symmetric and asymmetric PCR amplification. Selected aptamer pools are analyzed by flow cytometry and electrochemical detection. The best pool is cloned and sequenced.

PCR Amplification. Fifteen cycles of symmetric PCR, followed by 20 cycles of asymmetric PCR, were used for the amplification of single-stranded DNA after the elution of DNA from the beads. PCR was carried out in a Mastercycler pro S thermal cycler (Eppendorf, Ontario, Canada). In addition to the DNA template, 50 μL of the PCR reaction mixture contained 1x Green GoTaq Flexi buffer, 2.5 mM $MgCl_2$, 0.025 U μL^{-1} GoTaq Hot Start Polymerase (Promega Corp., U.S.), and 200 μM dNTPs. For the symmetric amplification, 300 nM of 6-FAM-labeled forward primer and 300 nM unlabeled reverse primer were used. However, for the asymmetric amplification, the concentration of the forward primer was 20 times higher than the concentration of the reverse primer (1 μM and 50 nM, respectively). The following settings were used for the thermal cycler: melting at 94 °C for 30 s, annealing at 56 °C for 15 s, and extending at 72 °C for 15 s.

Flow Cytometric Competitive Binding Assay. A total of 200 nM of each aptamer pool was mixed with 10 ng μL^{-1} of purified DyLight 488-conjugated anti-VSV polyclonal antibody (Rockland Inc., PA) and incubated for 1 h at room temperature. To this solution was added 6×10^8 PFUs of VSV, followed by incubation at 37 °C for 30 min, and subjection to flow cytometric analysis. Fluorescent antibodies allowed the identification of virus particles. The virus alone, antibody alone, and DPBS buffer were used as controls.

Aptamer Cloning and Sequencing. An aptamer pool was amplified by symmetric PCR using nonlabeled primers and purified with AxyPrep DNA Gel Extraction Kit (Axygen Biosciences, CA). The aptamer pool was then cloned into *E. coli* using the pETBlue-1 Perfectly Blunt Cloning Kit (Invitrogen, CA). Plasmids containing the insert were isolated from bacterial colonies with the GeneJET Plasmid Miniprep Kit (Thermo Fisher Scientific Inc., MA) and amplified by PCR. Their sequences were determined by Génome Québec (Canada).

Preparation of VSV Immunosensor. Prior to binding experiments, the gold electrode (2-mm diameter, CH Instruments, TX) was cleaned by oxidation and reduction scanning under basic conditions (scan rate, 2 V s^{-1}; in 0.5 M NaOH) over the potential range from −0.35 to −1.35 V (vs Ag/AgCl reference electrode saturated with 3 M NaCl). Next, the electrode was cyclically cleaned under acidic conditions (scan rate, 4 V s^{-1}; in 0.5 M H_2SO_4) over the potential range from −0.35 to −1.35 V. The scan was repeated, typically 1000 scans under basic conditions and 100 scans under acidic conditions. Afterward, the electrode was cleaned by sonication in absolute ethanol and dried with N_2. The cleaned gold electrode was incubated with 2 mM lipoic acid in ethanol for 24 h, at room temperature. Afterward, the electrode was incubated with 1-ethyl-3-[3-dimethylaminopropyl]-carbodiimide hydrochloride (EDC) in acetonitrile (1%, w/v) for 2 h followed by *N*-hydroxysuccinimide (NHS) in acetonitrile (1%, w/v) for 2 h, at room temperature. Consequently, the electrode was incubated with 0.5 mg mL^{-1} of the anti-VSV antibody in 10 mM sodium phosphate buffer, pH 7.4, overnight at 4 °C. The remaining active ester was quenched by incubating the Ab-modified electrode in 100 mM ethanolamine solution in ethanol for 1 h, at room temperature. Subsequently, the Ab-modified electrode was incubated with ethanolic 1 mM hexanethiol solution for 5 min to backfill the empty spots of the electrode surface, thus reducing the nonspecific hydrophobic protein adsorption on the surface.[11] Finally, the electrode was rinsed with ethanol and Millipore water to give the VSV-immunosensor.

Electrochemical Measurements. Electrochemical studies, including cyclic voltammetry (CV) and electrochemical impedance spectroscopy (EIS), were performed with an electrochemical analyzer

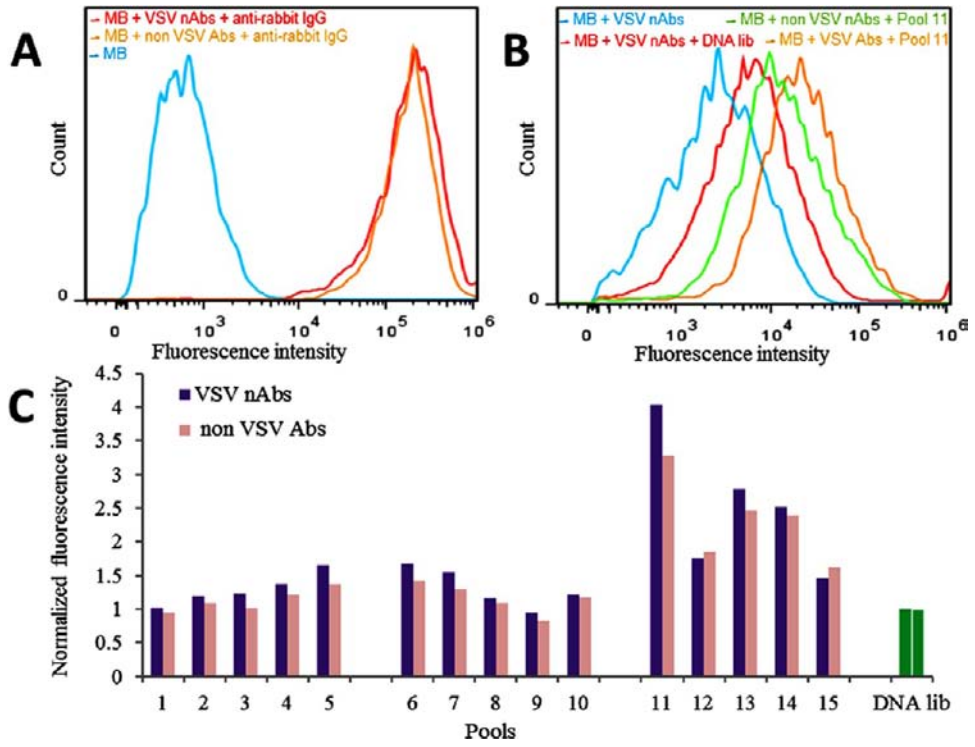

Figure 3. Flow cytometric analyses of DNA affinity to anti-VSV nAbs and nonspecific rabbit antibodies (non-VSV Abs). (A) Fluorescence of magnetic beads alone (MB, blue), and the beads incubated with Alexa Fluor 488 antirabbit IgG antibodies, showing the presence of anti-VSV nAbs (red) and non-VSV Abs (orange) on beads. (B) Representative histograms of binding affinity of fluorescent aptamer pool 11 to anti-VSV nAbs on beads (orange) and to non-VSV Abs on beads (green), and compared to the binding of the fluorescent DNA library to anti-VSV nAbs on beads (red). Beads with VSV Abs (blue) are presented as a control. (C) Comparative binding of fluorescent aptamer pools (150 nM) to anti-VSV nAbs (purple) and non-VSV antibodies (pink). The DNA library (150 nM, green) was used as a control and was also employed to normalize the fluorescence.

(CH Instruments 660D, TX) connected to a personal computer. All measurements were carried out at room temperature in an enclosed and grounded Faraday cage. A conventional three-electrode system was used, including the antibody-modified gold electrode as a working electrode, a platinum wire as a counter electrode, and Ag/AgCl/3 M NaCl as a reference electrode. The reference electrode was always isolated from the cell by a miniature salt bridge (agar plus KNO_3) to avoid the leakage of the Cl^- ions from the reference electrode to the measurement system. The open-circuit or rest-potential of the system was measured prior to all electrochemical experiments to prevent sudden potential-related changes in the SAM. CV experiments were performed at a scan rate of 100 mV s^{-1} in the potential range from −200 to 600 mV. EIS measurements were conducted in the frequency range from 100 kHz to 0.1 Hz, at a formal potential of 250 mV and AC amplitude of 5 mV. The measured EIS spectra were analyzed with the help of equivalent circuit using ZSimpWin 3.22 (Princeton Applied Research, U.S.), and the data were presented in Nyquist plots. All electrochemical measurements were performed in 20 mM Tris−ClO_4 buffer (pH 8.6), containing 2.5 mM $[Fe(CN)_6]^{3-/4-}$. All measurements were repeated for a minimum of three times with separate electrodes to obtain statistically meaningful results.

Cell-Based Viral Infectivity Assay. Aptamer-shielded nAbs were prepared by incubating 30 μL of nAbs-containing whole rabbit serum with 0.33 μL of 100 μM aptamers in DPBS for 1 h at 37 °C. Next, aptamer-binding nAbs were incubated with 30 μL of VSV (2×10^6 PFU) for 1 h at 37 °C. After that, the aptamer−nAb−virus mixture (60 μL) was serially diluted in 250 μL of serum-free medium and added to a Vero cell monolayer (0.4×10^6 cells per well) in a 12-well culture plate. The final concentration of aptamers was 132 nM per well. After incubation for 1 h at 37 °C in a 5% CO_2 humidified incubator (Thermo Fisher Scientific Inc., MA), all media were removed, and cells were overlaid with 1 mL of fresh 1% agarose dissolved in Dulbecco's Modified Eagle Medium (DMEM, Invitrogen, CA) supplemented with 10% Fetal Bovine Serum Sigma-Aldrich (Ontario, Canada). After 24 h of incubation, cells infected by VSV and positive for GFP fluorescence were visualized using Alfa Innotech Imaging System, Version 3.0.3.0. In addition, a standard plaque assay was performed, where the same plates were fixed with methanol−acetic acid fixative (3:1 ratio), stained with Coomassie Brilliant Blue R solution (Sigma-Aldrich, Ontario, Canada), and white plaques were counted.[10]

RESULTS AND DISCUSSION

Aptamer Selection. A modified SELEX method was used to select aptamers that bind to the Fab region of anti-VSV nAbs, as schematically represented in Figure 2. Coupling of nAbs with protein G-coated magnetic beads excluded the Fc region of nAbs from aptamer binding. We speculated that binding of protein G to the Fc region would hide it from aptamers. Furthermore, the use of magnetic beads provided a facile way of separating Fab-bound aptamers from unbound DNA. The first round of aptamer selection started with 3×10^{15} sequences of the DNA library. The library was first mixed with noncoated beads and incubated for 1 h at room temperature. After pulling the beads down by a magnet, the supernatant was collected and incubated with anti-VSV nAbs-coated beads for another hour. The beads were then pulled down, and the supernatant was removed and discarded. DNA aptamers bound to beads were washed and heated to collect the dissociated aptamers. To increase the low abundant aptamers, we amplified them initially by 15 cycles of symmetric PCR with equal concentration of primers. Subsequently, we performed additional 20 cycles of asymmetric PCR with an excess of a fluorescent forward primer. The asymmetric PCR had less

dx.doi.org/10.1021/ja306856y | J. Am. Chem. Soc. 2012, 134, 17168−17177

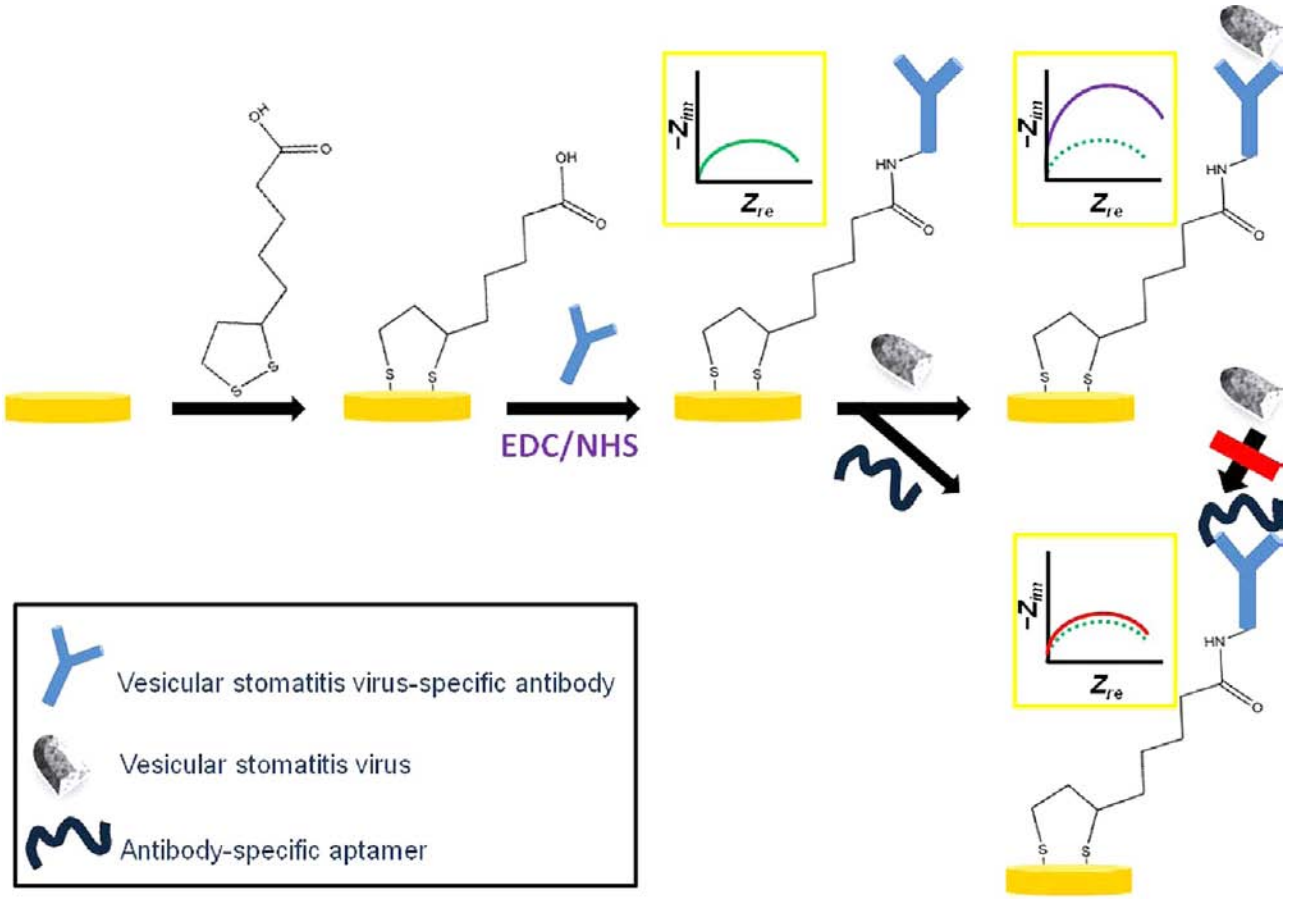

Figure 4. Electrochemical detection of AptaNAS. A self-assembled monolayer of lipoic acid is formed on the gold surface. Lipoic acid is then activated by incubation with 1-ethyl-3-[3-dimethylaminopropyl]carbodiimide hydrochloride (EDC) then *N*-hydroxysuccinimide (NHS) followed by coupling with the VSV-specific antibody. Subsequently, the surface is backfilled with 1-hexanethiol. The developed immunosensor is then employed for direct analysis of VSV. Alternatively, the immunosensor is treated with anti-Fab aptamers, and the modulation of the electrochemical signal is measured after comparison with the original signal given by the immunosensor (green curve) and VSV (purple).

amplification power but produced predominantly a pool of labeled single-stranded aptamers. The remaining PCR primers and dNTPs were removed with a 30 kDa molecular weight cutoff filter. The purification step concludes the first round of selection and results in an enriched aptamer pool, which will be used for subsequent selection. The next four rounds were done similarly, where we performed a positive selection to anti-VSV nAbs-coated beads followed by a negative selection step to protein G magnetic beads only. In rounds 6−10, the beads for negative selection were coupled with non-VSV antibodies. In rounds 11−15, two negative selection steps (beads alone and non-VSV Ab-coated beads) preceded the positive selection step. Binding of aptamers was analyzed by flow cytometry, and the selection was stopped after 15 rounds when no further increase of pool affinity to nAbs was observed (Figure 3).

In the first five rounds of selection, a constant increase of DNA affinity to nAbs was observed. However, when we introduced a negative selection to nonspecific antibodies, we observed a decrease of DNA affinity. This loss could be explained by elimination of aptamers to common structures among all antibodies. As we introduced the negative selections prior to the positive, the affinity of pools increased by more than 3-folds as compared to the native DNA library (Figure 3). Five pools with high affinity and specificity for anti-VSV antibody were tested in flow cytometric competitive binding assays. As seen in Figure S1, fluorescently labeled anti-VSV nAbs and nonlabeled aptamer pools were preincubated and then added to the virus. The complex of fluorescent antibody with the virus was monitored with the presence of different aptamer pools and DNA library as a control. The lowest fluorescence signal of nAbs−virus complex was an indication that pool 11 competed well with nAbs for binding the virus. On the basis of the affinity and antibody replacement results, pool 11 was chosen for the following cloning and sequencing to obtain individual aptamer clones. Subsequently, we designed an electrochemical immunosensor to confirm the binding of the clones to the Fab region of nAbs and the protection of the virus from neutralizing antibodies.

Electrochemical Characterization and Analytical Parameters of the VSV Immunosensor. The immunosensor is based on the formation of a self-assembled monolayer of lipoic acid onto the gold electrode.[12] Subsequently, nAbs were covalently coupled to the activated lipoic acid. The principle of the immunosensor is shown in Figure 4. It was employed for the detection of VSV via electrochemical impedance spectroscopy (EIS). As compared to other electrochemical methods, EIS has a less destructive effect on the measured biological interactions because it is performed at a very narrow range of small potentials.[13] The electrochemical characteristics of the fabricated immunosensor were investigated by cyclic voltammetry (CV) and EIS in the presence of 20 mM Tris−ClO_4 buffer (pH 8.6), containing 2.5 mM $[Fe(CN)_6]^{3-/4-}$. As shown

dx.doi.org/10.1021/ja306856y | *J. Am. Chem. Soc.* 2012, 134, 17168−17177

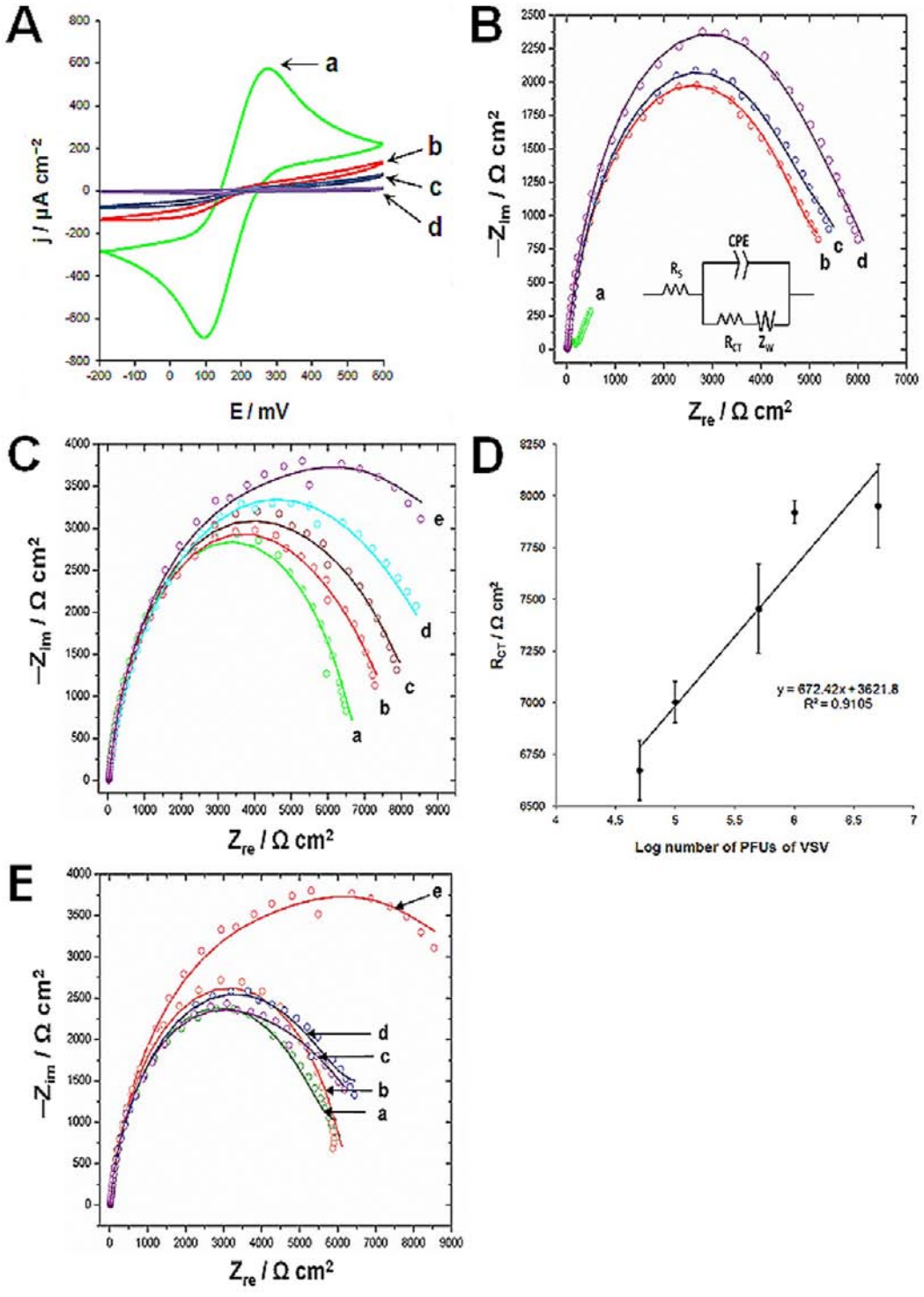

Figure 5. (A) Cyclic voltammograms and (B) Nyquist plot ($^{-}Z_{im}$ vs Z_{re}) of impedance spectra of the vaccinia virus immunosensor after each immobilization or binding step. The cyclic voltammograms were recorded at a scan rate of 100 mV s^{-1}, with (a) bare gold; (b) after formation of a self-assembled monolayer[12] of lipoic acid; (c) after covalent coupling of the VSV-specific antibody; and (d) after surface backfilling with 1 mM hexanethiol. The inset of (B) represents the circuit employed to fit to EIS measured data. The circuit consists of the ohmic resistance, R_S, of the electrolyte solution, resistance to charge transfer, R_{CT}, constant phase element, CPE, and Warberg impedance resulting for the diffusion of ions into the film, Z_W. (C) Nyquist plot ($^{-}Z_{im}$ vs Z_{re}) of impedance spectra obtained using (a) 0.5×10^5, (b) 10^5, (c) 0.5×10^6, (d) 10^6, and (e) 0.5×10^7 PFU mL^{-1} of VSV in DPBS after incubation with the developed immunosensor for 1 h at 37 °C. (D) Logarithmic plot of the number of VSV particles (PFU mL^{-1}) and the resistance to charge transfer, R_{CT}. (E) Selectivity experiments were performed using (a) buffer alone, (b) 0.5×10^7 PFU mL^{-1} of vaccinia virus, (c) 0.5×10^7 PFU mL^{-1} of VSV using vaccinia virus-specific antibody on the surface, (d) 5.1 mg mL^{-1} HSA, and (e) 0.5×10^7 PFU mL^{-1} of VSV. All were used in Dulbecco's phosphate buffered saline after incubation with the developed immunosensor for 1 h at 37 °C. The impedance spectra were recorded from 100 kHz to 0.1 Hz, and the amplitude was 0.25 V vs Ag/AgCl. All electrochemical measurements were performed in 20 mM TrisClO_4 buffer (pH 8.6), containing 2.5 mM $K_4[Fe(CN)_6]$ and 2.5 mM $K_3[Fe(CN)_6]$.

dx.doi.org/10.1021/ja306856y | J. Am. Chem. Soc. 2012, 134, 17168−17177

Table 1. Aptamer Sequences and DoS Values Measured by Electrochemical Immunosensor[a]

clone	sequence	degree of shielding, DoS %
C1L	CTCCTCTGACTGTAACCACGCCCAGAAACAGCACCCTTACATCGACTGGACCTTCCGCGGCATAGGTAGTCCAGAAGCC	35.9
C3L	CTCCTCTGACTGTAACCACGACTAGGACGCTTGGGAGGGGGGGTGGGGTGTCCGGTCGCGGCATAGGTAGTCCAGAAGCC	67.5
C5L	CTCCTCTGACTGTAACCACGTGTGCCAAAGAGAGTGGTGGGGGGGTGGGCGGAACTCGCGGCATAGGTAGTCCAGAAGCC	73.8
C9L	CTCCTCTGACTGTAACCACGACCGCCTTCCACCGTTCTCCACCACCCCTCAAACAACCCTGCATAGGTAGTCCAGAAGCC	66.2
C10L	CTCCTCTGACTGTAACCACGCCACCGAGCCTACCACATGTGACATCCCAGGACATAGCTGGCATAGGTAGTCCAGAAGCC	68.3
C1S	CCCAGAAACAGCACCCTTACATCGACTGGACCTTCCGCG	62.0
C3S	ACTAGGACGCTTGGGAGGGGGGGTGGGGTGTCCGGTCGCG	71.8
C4S	CCGGGGAATCTAGGGGAGGGCGGGTGGGTCAATTGAGCCG	61.7
C5S	TGTGCCAAAGAGAGTGGTGGGGGGGTGGGCGGAACTCGCG	70.4
C7S	CCAACCACACATCCTTCCATCGACATGGACCCACCGTTCC	27.7
C9S	ACCGCCTTCCACCGTTCTCCACCACCCCTCAAACAACCCT	34.5
C10S	CCACCGAGCCTACCACATGTGACATCCCAGGACATAGCTG	40.1

[a]L stands for a long DNA sequence, and S stands for a short DNA sequence.

in Figure 5A, the pretreated gold electrode presents a quasi-reversible voltammogram indicating that the redox reactions easily occurred on the bare gold surface, evidenced by very large redox currents (curve a). Formation of SAM of lipoic acid onto the gold surface substantially reduced the electrode current; also the sigmoidal behavior observed in curve b could be indicative of limited charge transfer via tunneling or diffusion through the defects in the formed layer.[14] The covalent coupling between the amino group of VSV-specific antibody and the activated lipoic acid brought about a further increase in the interfacial resistance (curve c) due to the low conductivity of proteins. Final treatment with hexanethiol greatly reduced the redox currents because they can penetrate down to the electrode surface, thereby blocking the direct access of the conducting ions (curve d). The Nyquist plots of the impedance spectra are shown in Figure 5B and corroborate the CV data (Figure 5A). The complex impedance was presented as the sum of the real Z, Z_{re}, and imaginary Z, Z_{im}, components that originate mainly from the resistance and capacitance of the cell, respectively.[15] A suitable equivalent circuit, shown in the inset of Figure 5B, was carefully selected to reflect the real electrochemical process and to enable fit producing accurate values.[16] The circuit includes the ohmic resistance, R_S, of the electrolyte solution, the electronic charge transfer resistance, R_{CT}, in series with the finite length Warburg W, and in parallel with a constant phase element, CPE, associated with the double layer, and reflects the interface between the assembled film and the electrolyte solution. The solution resistance, R_S, is the resistance between the antibody-modified gold electrode and the reference electrode. The high frequency semicircle of the Nyquist diagram corresponds to the charge transfer resistance, R_{CT}, in parallel with the CPE. The former represents the electron-transfer kinetics of the redox probe at the electrode surface, whereas the latter corresponds to a nonlinear capacitor accounting for the inhomogeneity of the formed film.[17] The diameter of the semicircle corresponds to the interfacial resistance at the electrode surface, the value of which depends on the dielectric and insulating features of the surface layer. On the other hand, the Warburg impedance, Z_W, accounts for a diffusion-limited electrochemical process, presumably due to molecular motions within the film caused by conducting ions penetration.[18] As shown in Figure 5B, the interfacial resistance increased after each step of immunosensor preparation, indicating a purely geometric effect on the surface.

Prior to titration experiments, aliquots containing different numbers of VSV particles,10^4, 0.5×10^5, 10^5, 0.5×10^6, 10^6, 0.5×10^7, and 10^7 PFU mL^{-1} in 20 μL of DPBS, were incubated with the developed immunosensor for 1 h at 37 °C. EIS was performed, and the numerical values for the circuit components were extracted at each aliquot, as shown in Figure 5C and Table S1. The rationale behind this electrochemical approach is that the binding between immobilized nAbs and free VSV will further block the charge transfer from a solution-based redox probe to the electrode surface. Consequently, R_{CT} will become increasingly high and can be used to monitor the binding event.[19] It was observed that the R_{CT} value increases linearly with the number of VSV particles, in the range from 0.5×10^5 to 0.5×10^7 PFU mL^{-1}, with the regression equation of $y = 672.42x + 3621.8$ ($R^2 = 0.9105$), where y is the R_{CT} value in Ω cm^2 and x is the logarithm of the number of VSV particles in PFU mL^{-1} as shown in Figure 5D. The relative standard deviation (RSD) values were between 0.7% and 2.8%. Beyond the upper VSV level, the response became nonlinear, indicating the saturation of the surface with the virus. The limit of detection (LOD) was 10^4 PFU mL^{-1}, estimated from $3(S_b/m)$, where S_b is the standard deviation of the measurement signal for the blank and m is the slope of the analytical curve in the linear region.[20] Control experiments were performed to reveal the selectivity and specificity of the recognition reaction. The results were compared to electrochemical signals obtained when the VSV immunosensor was incubated with either the buffer alone (5629.5 Ω cm^2, 0%) or 0.5×10^7 PFU mL^{-1} of VSV (7951 Ω cm^2, 100%). In one experiment, 5.1 mg mL^{-1} human serum albumin (HSA) gave 10.1% of the signal (5395 Ω cm^2). A second experiment was performed using 0.5×10^7 PFU mL^{-1} of another virus (vaccinia) instead of VSV, and the sensor gave 26.3% of the signal (6240 Ω cm^2). Using an immunosensor based on a nonspecific recognition element, antivaccinia nAb, resulted in only 16.2% of the signal (6007 Ω cm^2). As shown in Figure 5E, the results demonstrate the high selectivity of the developed immunosensor.

Degree of Shielding. An electrochemical immunosensor was developed to ensure that the selected aptamers can adequately shield the anti-VSV nAbs and thus can be further utilized to enhance VSV delivery into tumor cells. The developed biosensor was employed for screening of aptamers based on their degree of shielding (DoS) of the antibodies to find aptamer clones showing the highest shielding effect. The

dx.doi.org/10.1021/ja306856y | J. Am. Chem. Soc. 2012, 134, 17168−17177

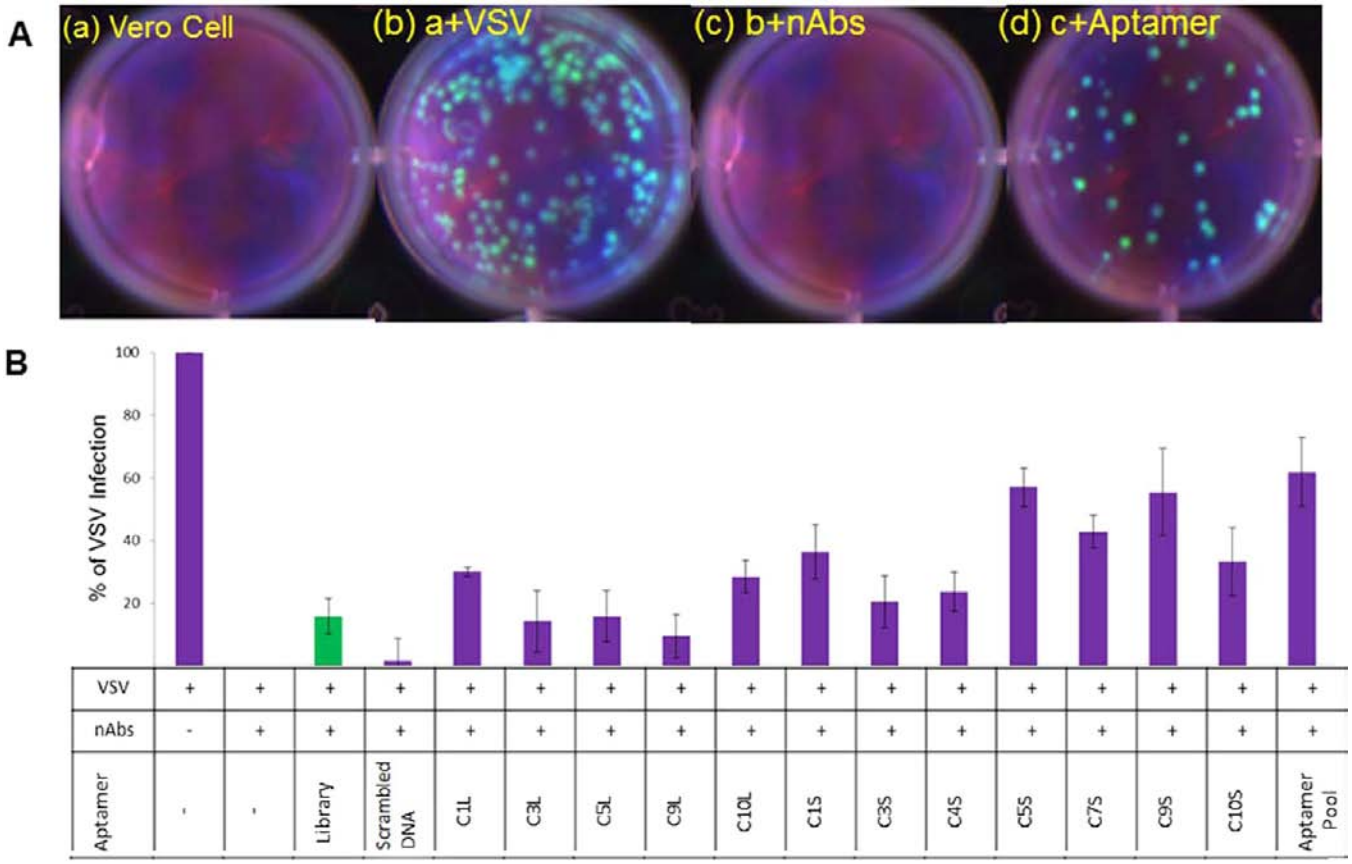

Figure 6. Viral infectivity cell-based assay. (A) (a) Vero cells only; (b) cells infected with VSV; (c) cells infected with VSV in the presence of nAbs; and (d) cells infected with VSV in the presence of nAbs and a representative aptamer pool. (B) Comparison of infection efficiencies of different aptamer clones and the pool, which consisted of an equimolar mixture of all aptamer clones.

evaluation is based on measuring the electrochemical signal resulted from the binding of VSV to aptamer-shielded immobilized nAbs when compared to the nonshielded counterpart. Briefly, the developed immunosensor was incubated with 20 μL of 100 μM aptamer clone in DPBS for 1 h at room temperature. After being rinsed with distilled water, the immunosensor was incubated with 0.5×10^7 PFU mL^{-1} of VSV (20 μL) for 1 h at 37 °C. EIS was performed and the R_{CT} baseline value was determined after the immunosensor preparation (R_{CTb}), after aptamer binding (R_{CTa}), and after the virus capture (R_{CTv}). Correspondingly, the change of R_{CT} upon virus binding (ΔR_{CTv}) was calculated for each aptamer-shielded anti-VSV nAbs by subtracting R_{CTb} from R_{CTv}. The reference ΔR_{CTv} value for the nonshielded anti-VSV nAbs was determined by incubating the immunosensor, without prior shielding, with VSV under the same incubation conditions. Hence, the DoS value can be calculated from the formula: DoS = (ΔR_{CTv} for nonshielded nAbs − ΔR_{CTv} for shielded nAbs)/ΔR_{CTv} for nonshielded nAbs (%). A control experiment was performed using the original DNA library instead of the aptamer clone. As can be seen in Figure S2, binding of VSV to the aptamer-shielded nAbs immobilized onto the gold surface caused a lower increase in interfacial resistance as compared to the nonshielded nAbs. The ΔR_{CTv} and the DoS values were calculated for each aptamer clone, and the results are shown in Table 1 and Table S2. Three aptamer clones (C5L, C3S, and C5S) have exhibited relatively high shielding effect (~70%). Importantly, the DNA library has demonstrated only a DoS value of 10.1%, indicating the high specificity of the aptamer clones and efficiency of aptamer selection technique.

Biological Activity of Aptamers in Vitro. To investigate the efficiency of the aptamers for shielding VSV from nAbs, cell-based experiments were performed. In these studies, we compared the infectivity of genetically modified VSV with nAbs shielded by the selected clones, as well as the DNA library and a scrambled DNA as controls. Briefly, aptamers were incubated with serum containing nAbs for 1 h at 37 °C; they were then mixed with VSV for an additional hour and added to a monolayer of Vero cells. After 1 h cells were washed, an agarose overlay in DMEM was added, and the plates were incubated overnight. The efficiency of aptamers was determined by fluorescent imaging of GFP expression in the infected Vero cells using a standard plaque assay and was compared for various clones (Figure 6). Neutralizing Abs completely inhibited cell infection by VSV, but addition of aptamers recovered the infectivity of virus. Clones C5S and C9S provide more than 50% recovery of VSV infection in the presence of nAbs in serum. C5S has also the highest DoS value in electrochemical biosensor. Interestingly, pooling of aptamer clones proved to have the highest shielding effect in cell experiments. This can be explained by the fact that VSV−nAbs are polyclonal, and a pool has the ability to block various paratopes via different clones of DNA aptamers.

■ CONCLUSION

For the first time, we have selected synthetic aptamers that bind to nAbs and shield oncolytic vesicular stomatitis virus and thus

dx.doi.org/10.1021/ja306856y | J. Am. Chem. Soc. 2012, 134, 17168−17177

allow an efficient infection of cells in the presence of nAbs. These aptamers have been seen to bind antibodies both in solution and immobilized on the surface of an electrochemical sensor. Flow cytometric and cell-based experiments were employed to screen aptamer clones against antibodies circulating in blood. Furthermore, we have shown that the clones bind to immobilized antibodies, mimicking the binding to antibodies on the surface of B lymphocytes. Shielding B cell receptors with administered aptamers could prevent the proliferation of B cells and thus inhibit the following production of nAbs against VSV. Aptamers have been tested for multiple in vivo applications, such as cell imaging,[21,22] drug delivery,[23,24] anticancer treatment,[25] and immunotherapy.[26] Some aptamers have undergone clinical evaluations like pegaptanib (marketed as Macugen), antinucleolin aptamer AS1411 with apoptotic induction activity in cancer cells,[27] and MOX-A12 targeting CCL2.[28] Two aptamers NU172 and RB006 bind and neutralize thrombin and blood coagulation factor IXa without serious adverse events.[29] Our anti-VSV aptamers have the potential to be administered with the oncolytic virus as a combined therapy for the first dose, and as a pretreatment, preceding the virotherapy, for the following doses. Thus, the aptamers can saturate the host neutralizing antibodies, and protect and increase circulation time of the oncolytic virus.

Furthermore, we used a bifunctional electrochemical immunosensor for quantitative analysis of VSV and for estimation of the shielding effect of selected aptamers. Several analytical techniques have been already applied for the detection of VSV, including ELISA, either by detection of VSV antibodies[30] or direct detection of VSV,[31] plaque assay,[32] RT-PCR,[33] and optical sensors.[34] However, our electrochemical immunosensor offers high sensitivity, selectivity, low cost, and short analysis time. The developed aptamers can also be used for designing an aptasensor, as previously explored by our group for the detection of viruses[35−37] and bacteria,[38] analyzing the presence of antiviral antibodies in blood, and profiling the immune status of a patient.

■ ASSOCIATED CONTENT

Supporting Information

Additional information as noted in text. This material is available free of charge via the Internet at http://pubs.acs.org.

■ AUTHOR INFORMATION

Corresponding Author

maxim.berezovski@uottawa.ca

Notes

The authors declare no competing financial interest.

■ ACKNOWLEDGMENTS

D.M. and M.L. contributed equally to this work. This work was supported by Strategic Project Grant #396508-10 from the Natural Sciences and Engineering Research Council of Canada (NSERC). We also thank Afnan Azizi and Mohamed Wehbe for critical reviews and valuable suggestions.

■ REFERENCES

(1) Breitbach, C. J.; Burke, J.; Jonker, D.; Stephenson, J.; Haas, A. R.; Chow, L. Q.; Nieva, J.; Hwang, T. H.; Moon, A.; Patt, R.; Pelusio, A.; Le Boeuf, F.; Burns, J.; Evgin, L.; De Silva, N.; Cvancic, S.; Robertson, T.; Je, J. E.; Lee, Y. S.; Parato, K.; Diallo, J. S.; Fenster, A.; Daneshmand, M.; Bell, J. C.; Kirn, D. H. *Nature* **2011**, *477*, 99−102.

(2) Mead, D.; Ramberg, F.; Besselsen, D.; Mare, C. *Science* **2000**, *287*, 486−487.

(3) Stojdl, D. F.; Lichty, B.; Knowles, S.; Marius, R.; Atkins, H.; Sonenberg, N.; Bell, J. C. *Nat. Med.* **2000**, *6*, 821−5.

(4) Balachandran, S.; Barber, G. N. *IUBMB Life* **2000**, *50*, 135−8.

(5) Fisher, K. D.; Seymour, L. W. *Adv. Drug Delivery Rev.* **2010**, *62*, 240−5.

(6) Doronin, K.; Shashkova, E. V.; May, S. M.; Hofherr, S. E.; Barry, M. A. *Hum. Gene Ther.* **2009**, *20*, 975−88.

(7) Ong, H. T.; Hasegawa, K.; Dietz, A. B.; Russell, S. J.; Peng, K. W. *Gene Ther.* **2007**, *14*, 324−33.

(8) Borghesi, L.; Milcarek, C. *Immunol. Res.* **2006**, *36*, 27−32.

(9) Stojdl, D. F.; Lichty, B. D.; tenOever, B. R.; Paterson, J. M.; Power, A. T.; Knowles, S.; Marius, R.; Reynard, J.; Poliquin, L.; Atkins, H.; Brown, E. G.; Durbin, R. K.; Durbin, J. E.; Hiscott, J.; Bell, J. C. *Cancer Cell* **2003**, *4*, 263−75.

(10) Diallo, J. S.; Vaha-Koskela, M.; Le Boeuf, F.; Bell, J. *Methods Mol. Biol.* **2012**, *797*, 127−40.

(11) Ayela, C.; Roquet, F.; Valera, L.; Granier, C.; Nicu, L.; Pugniere, M. *Biosens. Bioelectron.* **2007**, *22*, 3113−9.

(12) Eshoo, M. W.; Whitehouse, C. A.; Nalca, A.; Zoll, S.; Ecker, J. A.; Hall, T. A.; Pennella, T. T.; Duncan, D. D.; Desai, A.; Moradi, E. K.; Rudnick, K.; Libby, B.; Ranken, R.; Sampath, R.; Hofstadler, S. A.; Ecker, D. J.; Blyn, L. B. *PLoS One* **2009**, *4*, e6342.

(13) Bogomolova, A.; Komarova, E.; Reber, K.; Gerasimov, T.; Yavuz, O.; Bhatt, S.; Aldissi, M. *Anal. Chem.* **2009**, *81*, 3944−9.

(14) Su, L.; Gao, F.; Mao, L. *Anal. Chem.* **2006**, *78*, 2651−7.

(15) Yan, F.; Sadik, O. A. *J. Am. Chem. Soc.* **2001**, *123*, 11335−40.

(16) Bai, D.; Jennings, G. K. *J. Am. Chem. Soc.* **2005**, *127*, 3048−56.

(17) Dijksma, M.; Boukamp, B. A.; Kamp, B.; van Bennekom, W. P. *Langmuir* **2002**, *18*, 3105−3112.

(18) Baur, J.; Gondran, C.; Holzinger, M.; Defrancq, E.; Perrot, H.; Cosnier, S. *Anal. Chem.* **2010**, *82*, 1066−72.

(19) Mahmoud, K. A.; Kraatz, H. B. *Chemistry* **2007**, *13*, 5885−95.

(20) Bard, A. J.; Faulkner, L. R. *Electrochemical Methods: Fundamental and Applications*; Wiley: New York, 2001.

(21) Shi, H.; He, X.; Wang, K.; Wu, X.; Ye, X.; Guo, Q.; Tan, W.; Qing, Z.; Yang, X.; Zhou, B. *Proc. Natl. Acad. Sci. U.S.A.* **2011**, *108*, 3900−5.

(22) Gong, P.; Shi, B.; Zheng, M.; Wang, B.; Zhang, P.; Hu, D.; Gao, D.; Sheng, Z.; Zheng, C.; Ma, Y.; Cai, L. *Biomaterials* **2012**, *33*, 7810−7.

(23) Tong, G. J.; Hsiao, S. C.; Carrico, Z. M.; Francis, M. B. *J. Am. Chem. Soc.* **2009**, *131*, 11174−8.

(24) Chang, M.; Yang, C. S.; Huang, D. M. *ACS Nano* **2012**, *5*, 6156−63.

(25) Berezhnoy, A.; Stewart, C. A.; McNamara, J. O., II; Thiel, W.; Giangrande, P.; Trinchieri, G.; Gilboa, E. *Mol. Ther.* **2012**, *20*, 1242−50.

(26) McNamara, J. O.; Kolonias, D.; Pastor, F.; Mittler, R. S.; Chen, L.; Giangrande, P. H.; Sullenger, B.; Gilboa, E. *J. Clin. Invest.* **2008**, *118*, 376−86.

(27) Soundararajan, S.; Chen, W.; Spicer, E. K.; Courtenay-Luck, N.; Fernandes, D. J. *Cancer Res.* **2008**, *68*, 2358−65.

(28) Keefe, A. D.; Pai, S.; Ellington, A. *Nat. Rev. Drug Discovery* **2010**, *9*, 537−50.

(29) Chan, M. Y.; Rusconi, C. P.; Alexander, J. H.; Tonkens, R. M.; Harrington, R. A.; Becker, R. C. *J. Thromb. Haemostasis* **2008**, *6*, 789−96.

(30) Heo, E. J.; Lee, H. S.; Jeoung, H. Y.; Ko, H. R.; Kweon, C. H.; Ko, Y. J. *J. Virol. Methods* **2010**, *164*, 96−100.

(31) Kweon, C. H.; Kwon, B. J.; Kim, I. J.; Lee, S. Y.; Ko, Y. J. *J. Virol. Methods* **2005**, *130*, 7−14.

(32) Zhu, Y.; Warrick, J. W.; Haubert, K.; Beebe, D. J.; Yin, J. *Biomed. Microdevices* **2009**, *11*, 565−70.

(33) Rasmussen, T. B.; Uttenthal, A.; Fernandez, J.; Storgaard, T. *J. Clin. Microbiol.* **2005**, *43*, 356−62.

(34) Lopez, C. A.; Daaboul, G. G.; Vedula, R. S.; Ozkumur, E.; Bergstein, D. A.; Geisbert, T. W.; Fawcett, H. E.; Goldberg, B. B.; Connor, J. H.; Unlu, M. S. *Biosens. Bioelectron.* **2011**, *26*, 3432−7.
(35) Labib, M.; Zamay, A. S.; Muharemagic, D.; Chechik, A.; Bell, J. C.; Berezovski, M. V. *Anal. Chem.* **2012**, *84*, 1677−86.
(36) Labib, M.; Zamay, A. S.; Muharemagic, D.; Chechik, A. V.; Bell, J. C.; Berezovski, M. V. *Anal. Chem.* **2012**, *84*, 1813−16.
(37) Labib, M.; Zamay, A. S.; Muharemagic, D.; Chechik, A. V.; Bell, J. C.; Berezovski, M. V. *Anal. Chem.* **2012**, *84*, 2548−56.
(38) Labib, M.; Zamay, A. S.; Kolovskaya, O. S.; Reshetneva, I. T.; Zamay, G. S.; Kibbee, R. J.; Sattar, S. A.; Zamay, T. N.; Berezovski, M. V. *Anal. Chem.* **2012**, *84*, 8114−8117.